Dynamic Stability Problems Associated with Flare Stabilizers and Flap Controls

LARS ERIC ERICSSON* AND J. PETER READING†
Lockheed Missiles & Space Company, Sunnyvale, Calif.

As a rule, a flare is an effective stabilizing device used for ballistic re-entry, and the trailing edge flap provides efficient control of lifting re-entry. However, dynamic stability problems are caused by boundary-layer separation and/or bow-shock interaction with the aft body flowfield including bow shock interception of the flare or flap shock. A quasi-steady theory which lumps the effects of the motion time history to one discrete past time event is used to illustrate the various dynamic problems. Where experimental data have been available, good agreement has been found between experimental data and the theoretical predictions. However, many of the problems cannot be resolved by existing capabilities and further analytic and experimental efforts are needed.

Nomenclature‡

$C_{N\alpha}$ = $\partial C_N/\partial\alpha$
C_{M_q} = $\partial C_N/\partial(cq/U_\infty)$; $C_{N_{\dot\alpha}} = \partial C_N/\partial(c\dot\alpha/U_\infty)$
c = reference length, m (cylinder caliber for the flared body, body length for the lifting re-entry vehicle)
l = body length, m
M = Mach number
M_p = pitching moment, kg, coefficient $C_m = M_p/(\rho_\infty U_\infty{}^2/2)Sc$
N = normal force, kg, coefficient $C_N = N/(\rho_\infty U_\infty{}^2/2)S$
P = static pressure, kg/m²
q = rigid body pitch rate, rad/sec
S = reference area, m²(= $\pi c^2/4$ for the flared body, = projected plan form area for the lifting re-entry vehicle)
t = time, sec
U = axial velocity, m/sec
x = axial coordinate, m
α = angle of attack, rad or deg; $\dot\alpha = \partial\alpha/\partial t$
$\Delta\alpha$ = pitch oscillation amplitude, rad or deg
δ = wedge angle, rad or deg
Δ = difference
θ = surface slope, rad or deg
ξ = dimensionless x coordinate ($\xi = x/c$)
ρ = air density, kg-sec²/m⁴

Subscripts

F = flare
L = local, e.g., $C_{N\alpha_L}$ = force derivative with regard to local body attitude (α_L)
N = nose
EW = entropy wake effect
SS = shock-shock interaction effect
1,2,3 = numbering subscripts
∞ = freestream conditions

Superscripts

i = induced, e.g. $\Delta_{EW}{}^iC_N$ = normal force induced at the flare or flaps due to forebody changes (translatory position and/or cross flow)
$\bar\xi$ = aerodynamic center, e.g., $\bar\xi_F$ (a.c. of flare load)

Presented as Paper 69-182 at the AIAA 7th Aerospace Sciences Meeting, New York, January 20–22, 1969; submitted June 19, 1969; revision received October 20, 1969. The authors want to express their appreciation of the assistance given by N. Davis, I. Scholnick, and R. Guenther, in the numerical computations of Embedded-Newtonian Characteristics at angle of attack.

* Senior Staff Engineer. Associate Fellow AIAA.
† Research Specialist. Member AIAA.
‡ Also see Fig. 1.

Introduction

COMPRESSION surfaces have had wide usage as stability and control devices for entry vehicles. Flares have long been the standard stabilizing device for ballistic re-entry to subsonic terminal velocities, and present day lifting re-entry designs use trailing edge flaps of various types. Dynamic stability problems are associated with both devices. A quasi-steady theory which lumps the effects of the vehicle time history to one discrete past event has been used successfully to predict the transonic and hypersonic undamping contributions from the flare of blunt bodies of revolution.[1–3] The success of this simple analytic theory is due to the fact that it correctly accounts for the finite convection time between the generation of the nonuniform flowfield at the nose and the resulting modification of the flare load (see Fig. 1).

At transonic speeds, nose induced separation supplies the nonuniform flowfield over the flare (Fig. 2), whereas at hypersonic speed the entropy gradients caused by the curved bow shock generate the nonuniform flow (Fig. 3). The flare load component resulting from the nonuniform flowfield across the flare lags the body motion. As a result, the induced statically stabilizing load component is dynamically destabilizing. The similarity in the undamping results of the two nonuniform flowfields is apparent. A similar forebody dependence of the flare load exists when the bow shock interacts with the flare shock,[4] or when shock induced separation occurs.[5]

The flap-controlled lifting body experiences many of the same flow phenomena and must, as a consequence, experience many of the same dynamic stability problems as the flared body. In what follows, some of the potentially dangerous dynamic stability problems common to both geometries will be examined.

Discussion

Although the nonuniform flowfield effects are highly nonlinear, the method of local linearization can be used; i.e.,

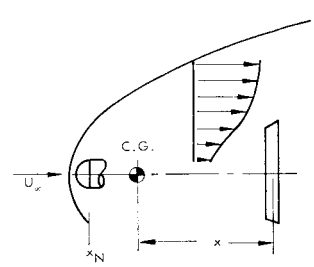

Fig. 1 Embedded-Newtonian flowfield.

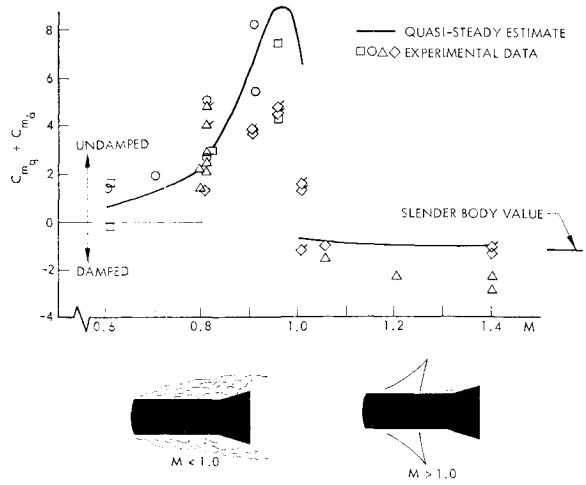

Fig. 2 Comparison between quasi-steady predictions and measured pitch damping for 1° amplitude oscillations around $\alpha = 0$ at $0.6 \leq M \leq 1.4$ (Ref. 1).

small perturbations from a steady-state (trim) condition are considered. The large amplitude perturbations can then be obtained using the small perturbation characteristics as functions of the (trim) angle of attack.[5]

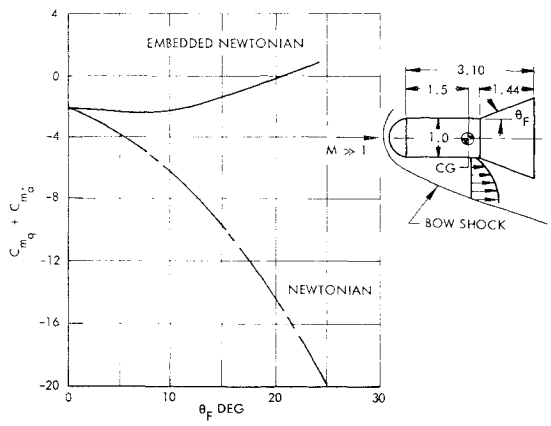

Fig. 3 Effect of flare angle on hypersonic vehicle damping.

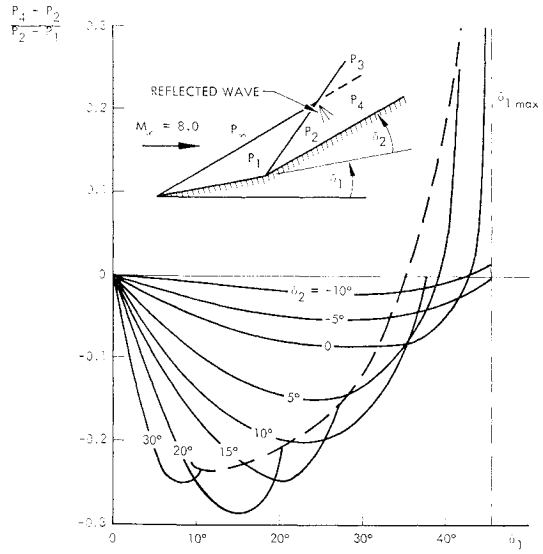

Fig. 4 Reflection pressure ratios for two wave interactions (Ref. 9).

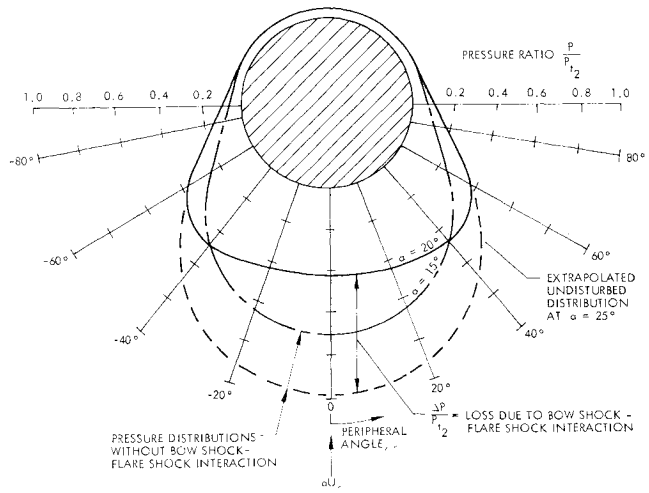

Fig. 5 Effect of bow shock/flare shock interaction on flare circumferential pressure distribution.

The bow shock-flare interaction at angle of attack represents the case where the axisymmetric body comes closest to simulating the flap controlled lifting re-entry vehicle, since the interaction effects are limited to the windward side.§ When the bow shock and flare or flap shock intersect, an expansion or a compression wave will be reflected from the intersection. Whether an expansion or a compression results depends upon the strength and relative inclination of the intersecting shock waves (Fig. 4).[6]

In the axisymmetric case, an expansion is the most likely result of the shock interaction, with the experimentally observed resultant pressure loss (Fig. 5) and unloading of the aft portion of the flare (Fig. 6). In the two-dimensional case a compression will often be the interaction result at high attitudes and flap deflections (see Fig. 7).[7-9]

Due to time lag, the shock interaction has opposite effects on static and dynamic stability. In the quasi-steady formu-

§ Otherwise, for the effects to be discussed later, the leeward side of the flared body gives sizable and sometimes dominant contributions.

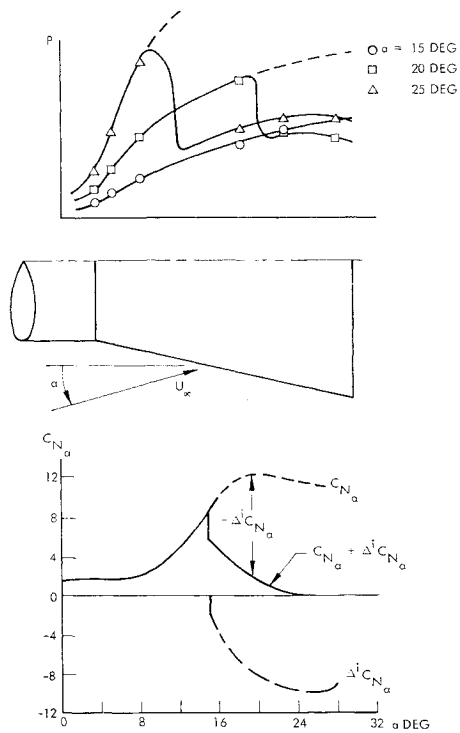

Fig. 6 Effect of bow shock/flare shock interaction on flare loads.

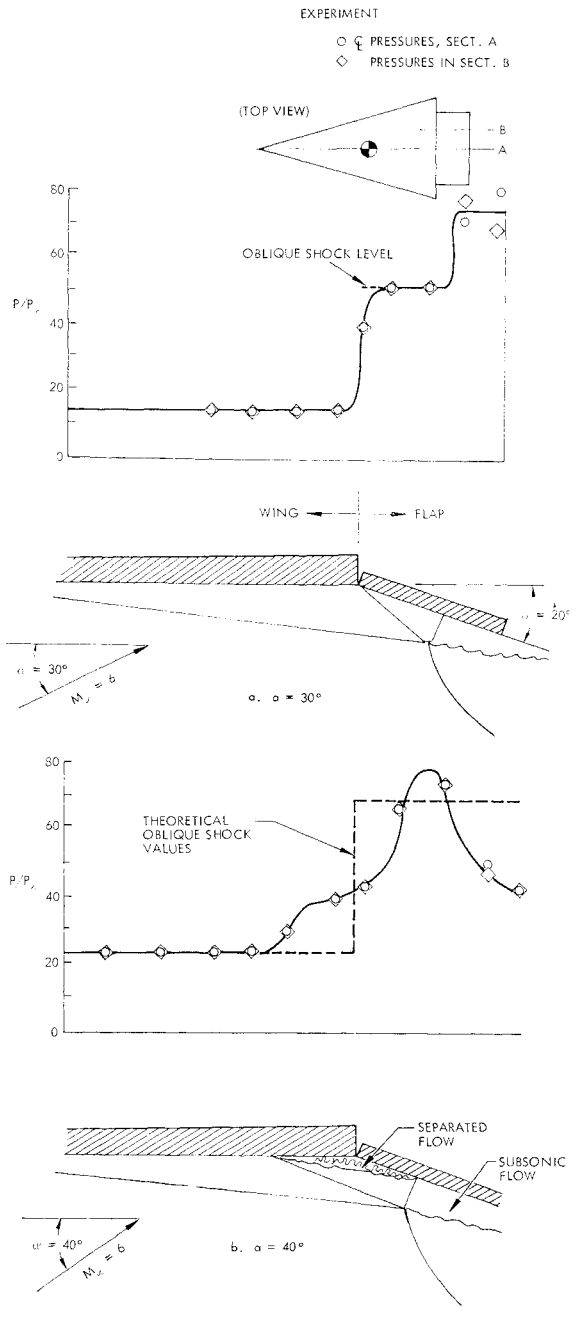

Fig. 7 Effect of bow shock/flap shock interaction on flap pressures (Ref. 9).

lation[2] the flare force derivatives in the "entropy wake" are

$$\left.\begin{aligned} C_{N\alpha_F} &= C_{N\alpha_L} + \Delta^i C_{N\alpha} \\ C_{N_{q_F}} &= \bar{\xi}_F C_{N\alpha L} \\ C_{N\dot{\alpha}_F} &= \xi_N \Delta_{EW^i} C_{N\alpha}/(\bar{U}/U_\infty) \end{aligned}\right\} \quad (1)$$

$\bar{U}/U_\infty$ is the integrated average velocity deficit over the flare. For the bow-shock flare-shock interaction the velocity ratio is unity, $\bar{U}/U_\infty = 1$.

The complete flare force derivatives at high angles of attack, where bow-shock flare-shock interaction occurs, can then be written as follows:

$$\left.\begin{aligned} C_{N\alpha_F} &= C_{N\alpha L} + \Delta_{EW^i} C_{N\alpha} + \Delta_{SS^i} C_{N\alpha} \\ C_{N_{q_F}} &= \bar{\xi}_F C_{N\alpha L} \\ C_{N\dot{\alpha}_F} &= \xi_N [\Delta_{EW^i} C_{N\alpha}/(\bar{U}/U_\infty) + \Delta_{SS^i} C_{N\alpha}] \end{aligned}\right\} \quad (2)$$

Subscripts EW and SS denote entropy-wake and shock-shock induced effects, respectively. $\Delta_{EW^i} C_{N\alpha}$ is always positive, whereas the shock interaction derivative $\Delta_{SS^i} C_{N\alpha}$ is negative for bodies with shallow flares or moderately deflected flaps, positive for very steep flares and large flap deflections (Fig. 4).[6]

Using the experimental data of Fig. 5 to define $\Delta_{SS^i} C_{N\alpha}$ gives flare force components that vary with angle of attack as shown in Fig. 8. The entropy gradient effect brings $C_{N\alpha F}$ up close to Newtonian values. However, due to time lag effects,[2] the dynamic contribution $\Delta_{EW^i} C_{N\dot{\alpha}}$ is undamping. Thus, $(C_{Nq_F} + C_{N\dot{\alpha}F})$ is very much below the Newtonian value and becomes even undamping at $\alpha \approx 7.5°$. The expansion-reaction of the shock-shock interaction reduces the static effectiveness of the flare but increases its dynamic effectiveness until it becomes dynamically stabilizing for $\alpha > 13°$.

The aerodynamic characteristics of the blunt-nose cylinder-flare body in Fig. 9 shows the large reduction in flare effectiveness that occurs at low α until the entropy gradient effects come into play at $\alpha \approx 15°$. Then the flare lift increases sharply until finally at $\alpha > 20°$, the expansion resulting from the bow-shock flare-shock interaction starts to reduce the flare force derivative (down toward Newtonian values). One would naturally suspect that flare induced flow separation[1] could have occurred in the wind tunnel test. However, the data do not indicate any such effects, and it could well be that the supersonic ($M \approx 4$) accelerated flowfield existing aft of the very blunt nose can negotiate the flare without any (extensive) separation.

If the flare is very steep, e.g., disk shaped,[1] or the flap is deflected at a large angle, the compression resulting from the shock interaction may produce the flap or flare characteristics¶ shown in Fig. 10. That is, the degradation of dynamic stability due to entropy gradient effects discussed earlier (Fig. 8) is aggravated by the shock interaction at $\alpha > 25°$, making the flare or flap contribution undamping for $25° < \alpha < 32°$. It is very likely that the load increase due to shock interaction is discontinuous,** as sketched in the figure.[5] There is no suitable experimental data available to demonstrate this hypersonic flow phenomenon. However, a very much similar flow phenomenon occurs on blunt re-entry

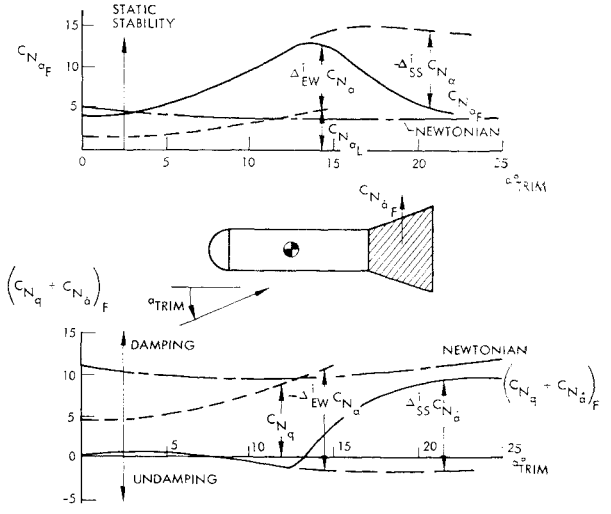

Fig. 8 Effects of entropy wake and bow shock/flare shock interaction on flare loads.

¶$\Delta_{SS^i} C_{N\alpha}$ in Fig. 10a is obtained from experimental data,[10] and the effect on damping is illustrated in Fig. 10b neglecting the entropy wake effect, i.e., with $\Delta_{EW^i} C_{N\alpha} = 0$.

** It may also be associated with (static) aerodynamic hysteresis effects.[5]

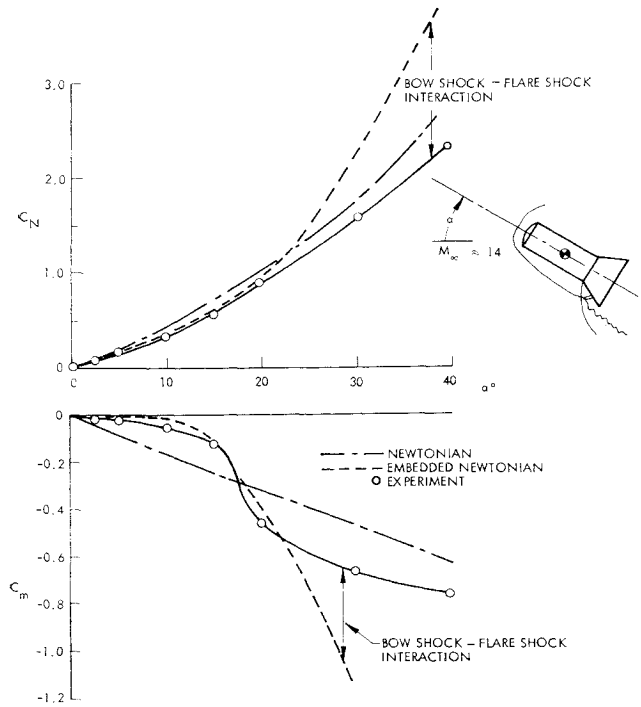

Fig. 9 Effect of bow shock/flare interaction on the aerodynamic characteristics of a blunt cylinder-flare body at $M_\infty = 14$.

capsules at transonic through hypersonic speeds[10] (Fig. 11). When the forebody wake attaches to the windward side of the aft body embedded in the wake (at $\alpha_d \geq 3.5°$) a discontinuous increase of static stability occurs. Due to the time lag existing between the time of the forebody crossflow change and the resulting wake movement, the dynamic effect is destabilizing, causing undamped 2° amplitude oscillations for $1.5° < \alpha_{TRIM} < 5.5°$. If the discontinuous moment change is large enough, oscillations around zero angle of attack can remain undamped up to large amplitudes. This is illustrated by a transonic separated flow phenomenon on blunt cylinder-flare bodies that exhibits the same type of discontinuity (Fig. 12). At slightly supersonic speeds the flow separates on the leeward side when $\alpha > \alpha_d$ and a discontinuous increase of the flare force results. Due to the time lag occurring before the nose generated separation reaches the flare to unload its leeward side, the statically stabilizing effect is undamping, and drives the vehicle dynamically unstable. Oscillations around $\alpha = 0$ are damped until the amplitudes become large enough to "catch" the leeward side separation. Then the oscillations become undamped and remain so up to large amplitudes ($\Delta\alpha_{LIMIT} \backsimeq 12°$). The phenomenon is dynamically similar to the bow-shock interaction with the flare or flap shock discussed earlier (Fig. 10). As the quasi-steady predictions, including time lag effects,[1] agree well with experimental data (Figs. 2 and 12), they should also give good predictions of the shock interaction effects, especially in view of the good agreement obtained between quadi-steady and Embedded-Newtonian theory in predicting "entropy wake" effects.[2]

The various flow phenomena discussed so far, i.e., entropy wake, shock-shock interaction, separation and reattachment, can all by themselves dramatically influence the vehicle dynamics. On a lifting, flap-controlled reentry vehicle they may all appear together.[7,8] Figure 13 illustrates what may happen at "incipient shock interception." The flap induced separation existing before shock intercept does, in general, not extend all the way back to the flap trailing edge, especially not with a flap design that allows span-wise venting of the separated flow pocket[7] (Fig. 14). However, when the strong shock resulting from the bow-shock flap-shock interac-

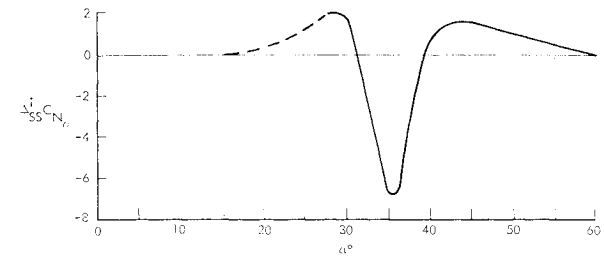

a) Load induced on flap vs α

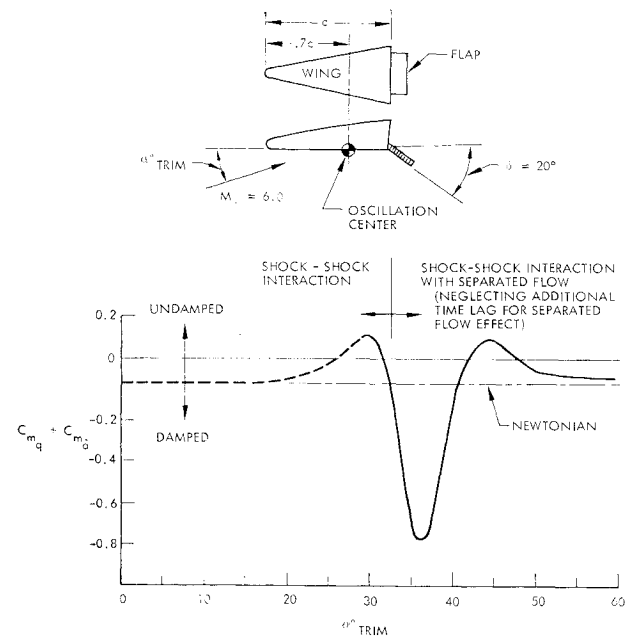

b) Damping vs α_{TRIM}

Fig. 10 Effect of bow shock/flap shock interaction on the aerodynamics of a lifting re-entry vehicle with delta wing plan form.

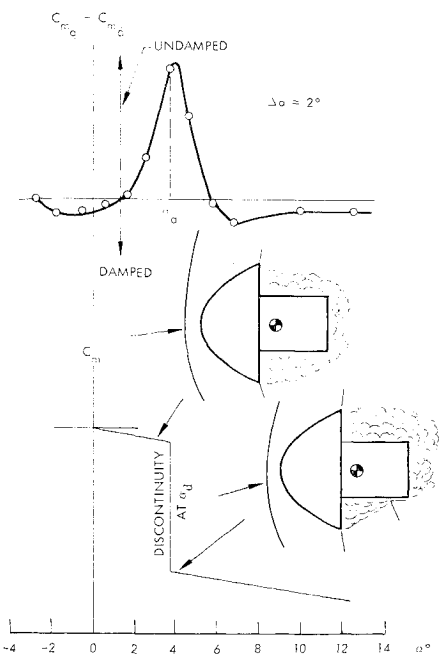

Fig. 11 Effect of tail load discontinuity on re-entry capsule stability.

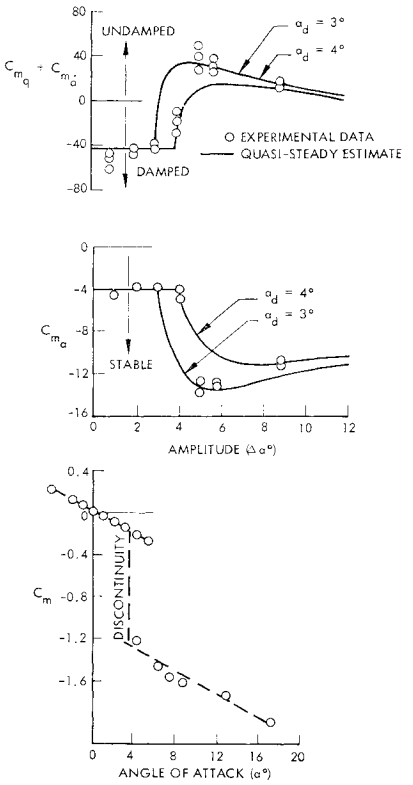

Fig. 12 Correlation of quasi-steady results with experiment for finite amplitude oscillations.

tion intercepts the flap, the resulting adverse pressure gradient causes the separation to extend all the way to the flap trailing edge (and the intercepting strong shock). As a result a force couple, $\Delta C_{N1} - \Delta C_{N2}$, is generated on the flap, as sketched in Fig. 13, and possibly also a positive body force ΔC_{N3}. This would cause the anomalous flap characteristics discussed by Markovin et al.[7,8] That is, the flap normal force decreases while the flap contribution to pitching moment continues to increase when the shock intercepts the flap. The dynamic consequences may be even more surprising. The bow-shock flap-shock interaction, which is associated with time lag effects, directs the flow separation change, which in turn has

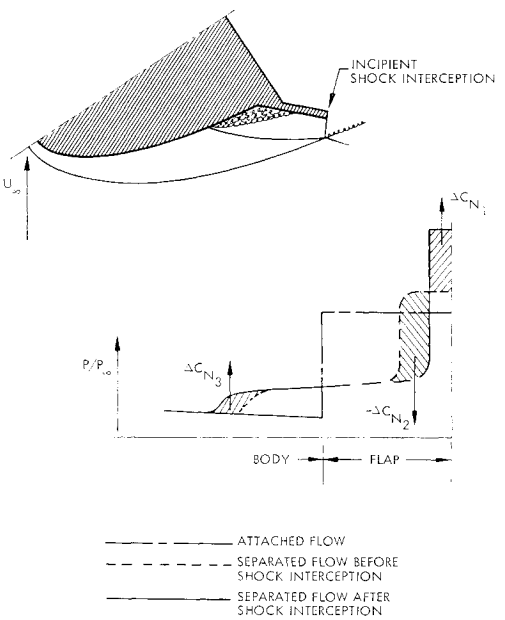

Fig. 13 Separation induced by bow shock/flap shock interaction.

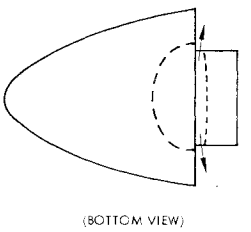

Fig. 14 Lateral venting of the flow separation pocket forward of a control flap.

its own time lag. The flap dynamics would be complicated by themselves, and when one considers the coupling between the flap control deflection and the rigid body motion, one recognizes that the problem may be serious. The flow shadowgraphs (Ref. 8 and sketch in Fig. 13), show a curved flap shock, amply demonstrating the existence of nonuniform flow, i.e., an entropy wake generated by the nose bluntness. Consequently, even before the shock-shock interaction some adverse dynamic coupling exists between the flap deflection and the body motion.[2] This is true even without the flap induced flow separation. With a flap design allowing venting of the separated flow pocket[7,8] (Fig. 14), the separation will probably not aggravate the body dynamics to any appreciable degree, especially not at higher Reynolds numbers.

All the aforementioned potential dynamic stability problems are more or less directly associated with a blunt nose. In many cases ballistic as well as lifting re entry vehicles will have an effectively blunt nosetip if the effects of viscosity, ablation, transpiration cooling, etc., are included. If the vehicle remains effectively sharp, one has to consider the effects of free body vortices at high angles of attack,[11] the strength of which are determined mainly by forebody crossflow,[12,13] but which induce the largest loads on aft body and fins, thus introducing large time lag effects to the vehicle dynamics. Maikapar[14] has demonstrated that this vortex interference effect exists also at hypersonic speeds. The bow shock can, of course, also interact with aft body fins or other protrusions, causing a variety of more or less powerful interactions.[15]

Conclusions

In view of what has been said, it is fair to draw the conclusion that the present state of the art is far from satisfactory when it comes to predicting the vehicle dynamics of existing and planned future re-entry vehicles. It is apparent that there are dynamic problems associated with flare stabilizers and flap controls, and that vehicles utilizing either of these devices should be analyzed carefully to make sure that the effects on vehicle dynamics are not unacceptable. Analytic theories, such as the Embedded-Newtonian theory or the quasi-steady theory accounting for time lag effects, could and should be extended to provide the insight needed for successful preliminary design of lifting re-entry vehicles.

References

[1] Ericsson, L. E. and Reding, J. P., "Dynamics of Separated Flow Over Blunt Bodies," LMSC 2-80-65-1, Contract NAS 8-5338, Dec. 1965, Lockheed Missiles & Space Co., Sunnyvale, Calif.

[2] Ericsson, L. E., "$\dot{\alpha}$-Effects Are Negligible at Hypersonic Speeds—Fact or Fiction?," paper RE76, Oct. 1968, 19th Congress of the International Astronautical Federation, New York.

[3] Ericsson, L. E., "Unsteady Aerodynamics of an Ablating Flared Body of Revolution Including Effects of Entropy Gradient," *AIAA Journal*, Vol. 6, No. 12, Dec. 1968, pp. 2395–2401.

[4] Fitzgerald, P. E., Jr., "On the Influence of Secondary Waves From the Intersection of Shocks of the Same Family," *Journal of the Aerospace Sciences*, Vol. 29, No. 6, June 1962, pp. 755–756.

[5] Ericsson, L. E., "Separated Flow Effects on the Dynamic Stability of Blunt-Nosed Cylinder-Flare Bodies," LMSC-667991, Contract NAS 9-5338, Dec. 1965, Lockheed Missiles & Space Co., Sunnyvale, Calif.

[6] Bird, G. A., "Effect of Wave Interactions on Pressure Dis-

tributions in Supersonic and Hypersonic Flow," *AIAA Journal*, Vol. 1, No. 3, March 1963, pp. 634–639.

[7] Markovin, M. V., Donohoe, J. C., and Larson, H. K., "Exploratory Investigations of the Effects of Gas Injection Through a Porous Model on Separation, Transition, Static Stability, and Control Effectiveness of a Blunt Entry Body at Mach number 7.3," AIAA Paper 68-27, New York, 1968.

[8] Markovin, M. V. and Donohoe, J. C., "Exploratory Investigations of the Effects of Gas Injection Through a Porous Model on Separation, Transition, Static Stability, and Control Effectiveness of a Blunt Entry Body at Mach number 7.3," Rept. ER 14598, Contract NAS 2-3873, July 1967, Martin Marietta Corp.

[9] Keyes, J. W. and Ashley, G. C., Jr., "Calculated and Experimental Hinge Moments on a Trailing-Edge Flap of a 75 Swept Delta Wing at Mach 6," TND-4268, Dec. 1967, NASA.

[10] Ericsson, L. E. and Reding, J. P., "Aerodynamic Effects of Bulbous Bases," CR-1339, Aug. 1969, NASA.

[11] Rainbird, W. J., "Turbulent Boundary-Layer Growth and Separation on a Yawed Cone," *AIAA Journal*, Vol. 6, No. 12, Dec. 1968, pp. 2410–2416.

[12] Tobak, M., Schiff, L. B., and Peterson, V. L., "Aerodynamics of Bodies of Revolution in Non-planar Motion," AIAA Paper 68-20, New York, 1968.

[13] Schiff, L. B., "A New Wind Tunnel Apparatus for Studying Coning and Spinning Motions of Bodies of Revolution," *Proceedings of the 3rd Technical Workshop on Dynamic Stability Problems*, NASA Ames Research Center, Nov. 1968.

[14] Maikapar, G. I., "Aerodynamic Heating of the Lifting Bodies," paper RE126, Oct. 1968, XIXth Congress of the International Astronautical Federation, New York.

[15] Edny, B., "Anomalous Heat Transfer and Pressure Distributions on Blunt Bodies at Hypersonic Speeds in the Presence of an Impinging Shock," FFA Rept. 115, Feb. 1968, The Aeronautical Research Institute of Sweden.

FEBRUARY 1970 J. SPACECRAFT VOL. 7, NO. 2

Flight Test Measurements of Boundary-Layer Transition on a Nonablating 22° Cone

M. M. SHERMAN* AND T. NAKAMURA†
Philco-Ford Corporation, Newport Beach, Calif.

Boundary-layer transition measurements were obtained on four flight tests of an experimental re-entry vehicle. The vehicle was a sharp, 22° half-angle cone with a beryllium heatshield and a graphite nose tip. Thermocouples and pressure taps were located on the cone surface and aft cover. Telemetered data were clear and consistent from flight to flight. The measured temperature histories agreed with preflight predictions during the period of laminar flow, and boundary-layer transition was clearly observed on all of the sensors. The transition process consisted of transitional flow which moved forward along the surface at a relatively fast rate, followed by the sudden occurrence of fully turbulent flow over the entire vehicle. The base temperature and pressure measurements verified the cone surface transition events. However, the base to freestream pressure ratios recorded during turbulent flow were significantly higher than have previously been reported for flight tests of more slender re-entry vehicles.

Nomenclature

C_f = local skin-friction coefficient
h = enthalpy
Re_X = Reynolds number based on wetted length
Re_θ = Reynolds number based on boundary-layer momentum thickness
u = velocity
x = surface distance
ρ = gas density

Subscripts

e = edge of boundary layer
r = recovery
w = wall

Introduction

PREFLIGHT predictions of boundary-layer transition are important to the design of many re-entry vehicles. As a result, many theoretical and experimental studies of this subject have been performed in recent years.[1–7] The objective of most of these experimental programs is to isolate and evaluate the effects of the many individual parameters that are known to influence transition. However, interpretation of these ground-test data is complicated by the fact that conditions associated with the test facility operation may also influence the transition process. The extent and magnitude of these effects are not always known. Therefore, controlled flight test measurements are the most desirable means of obtaining transition data, and offer the additional advantage of permitting evaluation of the more easily obtained ground-test results.

Most re-entry vehicles are designed for high performance flight and must necessarily use ablative heatshields. These vehicles sometimes contain instrumentation from which it is possible to obtain useful measurements of boundary-layer transition. Unfortunately, the effects of mass injection from the ablating surface cannot be uncoupled from these flight results. For purposes of obtaining a more basic understanding of the transition phenomena, it is desirable to obtain direct flight test measurements in the absence of mass transfer.

The present flight test program employed four identical conical vehicles with nonablating heatshields. These vehicles were instrumented to obtain accurate measurements of the cone surface temperature histories at several axial locations,

Presented as Paper 68-1152 at the AIAA Vehicle Systems and Technology Meeting, Williamsburg, Va., December 3–5, 1968; submitted February 6, 1969; revision received October 13, 1969.

* Supervisor, Thermodynamics Unit, Space and Re-Entry Systems Division. Member AIAA.

† Senior Engineering Specialist, Space and Re-Entry Systems Division.